ammonium ions. The shortest distances of the H atoms to O atoms are 2·330 (7), 2·299 (4) Å for one orientation of the ammonium ion, compared to 2·395 (4), 2·236 (5) Å for the other. These distances tend to the upper limit of ~2·38 Å for H···O bonding (Hamilton & Ibers, 1968) and would not preclude the apparent large thermal vibrational motion of the ammonium ion obtained.

We thank Dr K. Österlund for preparing the deuterated ammonium nitrate, the French Government (BWL) and the Finnish Academy (MA) for their support, and the ILL for making all facilities available to us.

References

Ahtee, M., Kurki-Suonio, K., Lucas, B. W. & Hewat, A. W. (1979). *Acta Cryst.* A**35**, 591–597.

Amorós, J. L., Arrese, F. & Canut, M. (1962). *Z. Kristallogr.* **117**, 92–107.

Burns, D. M., Ferrier, W. G. & McMullan, J. T. (1967). *Acta Cryst.* **22**, 623–629.

Busing, W. R. & Levy, H. A. (1964). *Acta Cryst.* **17**, 142–146.

Choi, C. S., Mapes, J. E. & Prince, E. (1972). *Acta Cryst.* B**28**, 1357–1361.

Goodwin, T. H. & Whetstone, J. (1947). *J. Chem. Soc.* pp. 1455–1461.

Hamilton, W. C. & Ibers, J. A. (1968). *Hydrogen Bonding in Solids.* New York: Benjamin.

Hewat, A. W. (1973). UKAEA Research Group Report R-7350 (unpublished).

Juopperi, O. (1972). *Ann. Acad. Sci. Fenn. Ser. A*6, **383**, 1–18.

Lucas, B. W., Ahtee, M. & Hewat, A. W. (1979). *Acta Cryst.* B**35**, 1038–1041.

Nagatani, M., Seiyama, T., Sakiyama, M., Suga, H. & Seki, S. (1967). *Bull. Chem. Soc. Jpn*, **40**, 1833–1844.

Rietveld, H. M. (1969). *J. Appl. Cryst.* **2**, 65–71.

Acta Cryst. (1980). B**36**, 2008–2011

Structure of Europium(II) Tetraborate

By Ken-Ichi Machida, Gin-Ya Adachi* and Jiro Shiokawa

Department of Applied Chemistry, Faculty of Engineering, Osaka University, Yamadakami, Suita-Shi, Osaka-fu 565, Japan

(*Received* 24 *January* 1980; *accepted* 1 *April* 1980)

Abstract

EuB_4O_7 is orthorhombic, space group $Pnm2_1$, with $Z = 2$, $a = 4{\cdot}435$ (1), $b = 10{\cdot}731$ (1) and $c = 4{\cdot}240$ (1) Å. The structure was refined to $R = 0{\cdot}023$ for 510 observed reflections with isotropic thermal parameters. The structure framework consists of a three-dimensional $(B_4O_7)_\infty$ network of BO_4 tetrahedra. Each Eu atom is surrounded by nine O atoms with Eu—O distances from 2·531 to 2·841 Å to form an EuO_9 polyhedron. The mean interatomic distances between Eu nearest neighbors and between Eu next-nearest neighbors are 4·338 and 6·171 Å, respectively. The thermal, magnetic and luminescence properties of EuB_4O_7 were found to be closely related to its crystal structure.

Introduction

Compounds containing divalent europium (Eu^{2+}) have been synthesized because of their magnetic and spectroscopic properties. Since the Eu^{2+} ion exists in a divalent state under a limited condition (McCarthy & White, 1970), no Eu^{2+}-containing compound has been obtained as a natural product. Recently we have prepared a series of Eu^{II} borates, $Eu_3B_2O_6$, $Eu_2B_2O_5$, EuB_2O_4 and EuB_4O_7, by the solid-state reaction of appropriate amounts of Eu_2O_3, B (metal) and H_3BO_3, and their magnetic and luminescence properties have been studied (Hata, Adachi & Shiokawa, 1977; Machida, Hata, Okuno, Adachi & Shiokawa, 1979; Machida, Adachi & Shiokawa, 1979*a*). The borates EuB_4O_7 and $Eu_2B_2O_5$ are paramagnetic, while EuB_2O_4 and $Eu_3B_2O_6$ are an antiferromagnet with $T_N = 3$K and a ferromagnet with $T_c = 7{\cdot}5$ K respectively. The tetraborate, EuB_4O_7, gives a band emission based on the $4f^7$–$4f^6\,5d$ transition of the Eu^{2+} ion.

In this paper we report the structure of EuB_4O_7 and discuss its thermal, magnetic and luminescence properties on the basis of the X-ray analysis.

Experimental

Single crystals were grown by the Bridgeman technique as follows: The polycrystalline EuB_4O_7 powder was

---

* To whom correspondence should be addressed.

0567-7408/80/092008-04$01.00 © 1980 International Union of Crystallography

Table 1. *Crystal data for* EuB_4O_7

FW 307·20	$\lambda = 0{\cdot}71069$ Å
Orthorhombic	μ(Mo $K\alpha$) = 15·54 mm^{-1}
Space group $Pnm2_1$	$D_m = 5{\cdot}01$ Mg m^{-3}
$a = 4{\cdot}435$ (1) Å	$D_x = 5{\cdot}06$
$b = 10{\cdot}731$ (1)	$Z = 2$
$c = 4{\cdot}240$ (1)	$F(000) = 278$
$V = 201{\cdot}8$ (2) Å^3	Crystal size 0·30 × 0·20 × 0·20 mm

packed into an iron crucible (8 mmø × 70 mm) and sealed in a silica tube in vacuum, and then introduced into a furnace which was allowed to cool from 1323 to 1173 K at a cooling rate of about 5 K h^{-1}. Pale-gray prismatic crystals were obtained.

Preliminary Weissenberg photographs showed that the crystals belonged to the orthorhombic system, and the observed systematic absences $k + l = 2n + 1$ for $0kl$ correspond to the space groups $Pnmm$ and $Pnm2_1$. The accurate cell parameters (Table 1) were determined by a least-squares treatment of the X-ray powder pattern (Cu $K\alpha$) calibrated with high-purity Si as an internal standard. The intensity data were measured on a Rigaku Denki automated four-circle diffractometer with Mo $K\alpha$ radiation monochromated by a graphite plate. The ω–2θ scan method was employed with a scanning rate of 4° min^{-1}. All possible reflections $\bar{h}k\bar{l}$ and $\bar{h}kl$ were collected out to $2\theta = 70°$. Three standard reflections were monitored every 50 reflections and no apparent decay in intensity was detected. The intensities of equivalent reflections were averaged and 510 unique reflections with $|F_o| \geq 3\sigma(|F_o|)$ were considered as observed. The standard Lorentz and polarization corrections were applied but no absorption correction was made.

Differential thermal analysis (DTA) and thermogravimetric analysis (TGA) were made on a Rigaku Denki DTA 'Thermoflex' in air at 298–1223 K and the heating rate was 10 K min^{-1}.

Structure determination

The structure was solved by the conventional heavy-atom method and refined with *HBLS*-V (Ashida, 1973) by the block-diagonal least-squares method, the function minimized being $\sum w(|F_o| - |F_c|)^2$. From a three-dimensional Patterson synthesis, the non-centrosymmetric space group $Pnm2_1$ was adopted and the Eu atom was determined to be on a set of special positions, 2(a): x,0,0 with $x = 0{\cdot}12$. The remaining atoms (O and B) were located on successive Fourier maps: O(1) at the 2(a) site and the other atoms at general positions [4(b) sites]. Isotropic refinements for all atomic parameters gave $R = 0{\cdot}023$ and $R_w = 0{\cdot}030$ for 510 observed reflections, where $R = \sum ||F_o| - |F_c|| / \sum |F_o|$ and $R_w = [\sum w(|F_o| - |F_c|)^2 / \sum w(F_o)^2]^{1/2}$. The atomic scattering factors for Eu, O and B were those in *International Tables for X-ray Crystallography* (1974). The weighting scheme $w = (F_m/F_o)^2$ for $F_o > F_m(=20{\cdot}0)$ and $w = 1{\cdot}0$ for $F_o \leq F_m(=20{\cdot}0)$ was employed to determine the coordinates of the light atoms more accurately. The final positional and thermal parameters are listed in Table 2.*

Table 2. *Final positional and thermal parameters*

Standard deviations are given in parentheses.

	x	y	z	B (Å^2)
Eu	0·2116 (3)	0	0	0·18 (1)
O(1)	0·768 (6)	0	0·581 (7)	0·31 (8)
O(2)	0·358 (4)	0·141 (4)	0·546 (4)	0·25 (5)
O(3)	0·727 (4)	0·135 (5)	0·134 (5)	0·31 (5)
O(4)	0·132 (5)	0·278 (4)	0·139 (5)	0·27 (5)
B(1)	0·672 (5)	0·122 (5)	0·463 (7)	0·28 (8)
B(2)	0·178 (5)	0·251 (5)	0·484 (14)	0·47 (8)

Table 3. *Interatomic distances* (Å) *and angles* (°) *in* EuB_4O_7

Standard deviations are given in parentheses.

(a) The $(B_4O_7)_\infty$ network

B(1)-tetrahedron		B(2)-tetrahedron	
B(1)–O(1)	1·465 (10)	B(2)–O(2)	1·449 (14)
–O(2)	1·451 (8)	–O(3^{i})	1·436 (15)
–O(3)	1·427 (8)	–O(4)	1·503 (14)
–O(4^{i})	1·573 (8)	–O(4^{ii})	1·556 (14)
Average	1·479	Average	1·486
O(1)–B(1)–O(2)	108·8 (6)	O(2)–B(2)–O(3^{i})	116·9 (10)
O(1)–B(1)–O(3)	111·9 (6)	O(2)–B(2)–O(4)	114·0 (10)
O(1)–B(1)–O(4^{i})	106·8 (6)	O(2)–B(2)–O(4^{ii})	104·3 (9)
O(2)–B(1)–O(3)	113·0 (6)	O(3^{i})–B(2)–O(4)	108·1 (9)
O(2)–B(1)–O(4^{i})	108·7 (5)	O(3^{i})–B(2)–O(4^{ii})	103·8 (9)
O(3)–B(1)–O(4^{i})	107·4 (5)	O(4)–B(2)–O(4^{ii})	109·1 (9)
Average	109·4	Average	109·4

(b) Eu–Eu distances

Nearest neighbors		Next-nearest neighbors	
Eu–Eu$^{\mathrm{i}}$	4·240 (1) (×2)	Eu–Eu$^{\mathrm{iii}}$	6·136 (1) (×4)
–Eu$^{\mathrm{ii}}$	4·435 (1) (×2)	–Eu$^{\mathrm{iv}}$	6·311 (1) (×4)
Average	4·338	–Eu$^{\mathrm{v}}$	6·067 (1) (×4)
		Average	6·171

(c) Eu–O distances

Eu–O(1^{i})	2·651 (7)	Eu–O(3)	2·768 (5) (×2)
–O(2)	2·841 (4) (×2)	–O(3^{ii})	2·653 (5) (×2)
–O(2^{i})	2·531 (4) (×2)	Average	2·693

Symmetry code: Eu$^{\mathrm{i}}$ (x, 0, ± 1), Eu$^{\mathrm{ii}}$ ($\pm 1 + x$, 0, 0), Eu$^{\mathrm{iii}}$ ($\pm 1 + x$, 0, ± 1), Eu$^{\mathrm{iv}}$ (x, $\pm\frac{1}{2}$, $\pm\frac{1}{2}$), Eu$^{\mathrm{v}}$ ($1 - x$, $\pm\frac{1}{2}$, $\pm\frac{1}{2}$), O(1^{i}) ($-1 + x$, 0, $-1 + z$), O(2^{i}) (x, $\pm y$, $-1 + z$), O(3^{i}) ($-x$, $\frac{1}{2} - y$, $\frac{1}{2} + z$), O(3^{ii}) ($-1 + x$, $\pm y$, z), O(4^{i}) ($1 - x$, $\frac{1}{2} - y$, $\frac{1}{2} + z$), O(4^{ii}) ($-x$, $\frac{1}{2} - y$, $\frac{1}{2} + z$).

---

* A list of structure factors has been deposited with the British Library Lending Division as Supplementary Publication No. SUP 35317 (3 pp.). Copies may be obtained through The Executive Secretary, International Union of Crystallography, 5 Abbey Square, Chester CH1 2HU, England.

Results and discussion

The interatomic distances and angles are summarized in Table 3 and the projections of the EuB_4O_7 structure viewed along the c and a axes are shown in Figs. 1 and 2. Eu and O(1) are located on mirror planes, $y = 0$ and $y = \frac{1}{2}$. There are two kinds of borate units, $B(1)O_4$ and $B(2)O_4$, with mean B–O distances 1·479 and 1·486 Å respectively and mean O–B–O angle 109·4°. The structure consists of a three-dimensional $(B_4O_7)_\infty$ network in which the $B(1)O_4$ and $B(2)O_4$ tetrahedra are alternately linked by sharing cornered O atoms. The Eu atoms are located in a so-called 'cage' formed by the BO_4 units of the $(B_4O_7)_\infty$ network and have four nearest and twelve next-nearest neighboring Eu atoms with mean interatomic distances 4·338 and 6·171 Å. Each Eu atom is surrounded by nine O atoms at individual distances varying from 2·531 to 2·841 Å to form an EuO_9 polyhedron (Fig. 3).

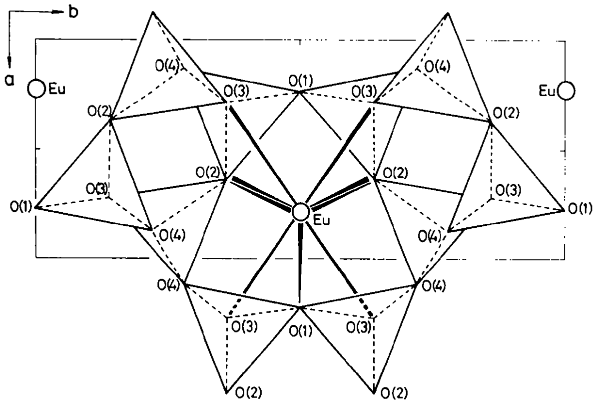

Fig. 1. A projection of the EuB_4O_7 structure viewed along the c axis.

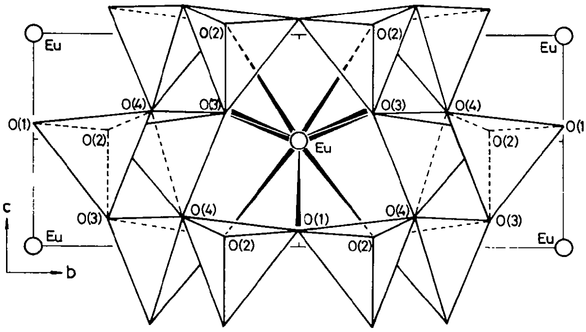

Fig. 2. A projection of the EuB_4O_7 structure viewed along the a axis.

The Eu^{2+} ions in solid phases of inorganic compounds are easily oxidized to Eu^{3+} ions by heating in an oxidizing atmosphere at 573–773 K (Felsche & Kaldis, 1972). The thermal analytical data for a series of Eu^{II} borates are presented in Fig. 4 and Table 4. The oxidation temperature is about 673 K for $Eu_3B_2O_6$, 683 K for $Eu_2B_2O_5$, 753 K for EuB_2O_4 and 1033 K for EuB_4O_7. The proportions of weight gains by oxidation are in good agreement with the corresponding theoretical values. It is noticeable that the oxidation temperature of EuB_4O_7 is considerably higher than those of other Eu^{II} borates. This can be considered as being attributable to their structural frameworks: From IR spectra and X-ray analyses (Machida, Hata, Okuno, Adachi & Shiokawa, 1979; Machida, Adachi & Shiokawa, 1979*b*), $Eu_3B_2O_6$ and $Eu_2B_2O_5$ contain BO_3^{3-} and $B_2O_5^{4-}$ ions respectively, and EuB_2O_4 consists of $(BO_2)_\infty$ chains. Their Eu^{2+} ions are closely packed together with the borate ions or along the direction of borate chains. The Eu^{2+} ions in EuB_4O_7 are completely surrounded by the BO_4 units of the $(B_4O_7)_\infty$ network, and are therefore hardly expected to be attacked by oxygen.

The magnetism of Eu^{II} compounds is interpreted from the magnitude of magnetic exchange and superexchange interactions *via* the overlap of $4f$ and $5d$ orbitals between nearest and next-nearest neighboring Eu^{2+} ions (McGuire & Shafer, 1964; McGuire, Shafer, Joenk, Alperin & Pickart, 1966), which is a

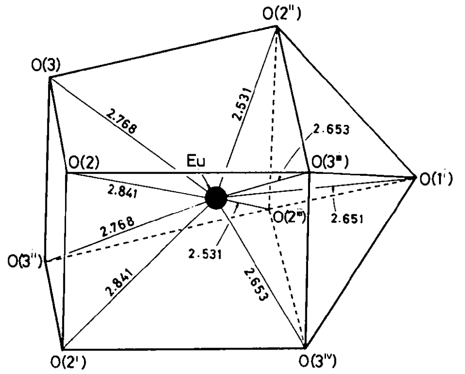

Fig. 3. A schematic illustration of the EuO_9 polyhedron in EuB_4O_7. The numerical values represent Eu–O nearest-neighbor distances (Å).

Table 4. *Structural and thermal data for* Eu^{II} *borates*

Compound	Symmetry	Structural framework	m.p. (K)	Oxidation temperature (K)	Weight gain (%) Found	Weight gain (%) Calcd.
$Eu_3B_2O_6$	Hexagonal	BO_3^{3-} ion	–	673	4·14	4·18
$Eu_2B_2O_5$	Monoclinic	$B_2O_5^{4-}$ ion	≃1270	683	3·88	3·95
EuB_2O_4	Orthorhombic	$(BO_2)_\infty$ chain	≃1270	753	3·33	3·37
EuB_4O_7	Orthorhombic	$(B_4O_7)_\infty$ network	1258	1033	2·51	2·60

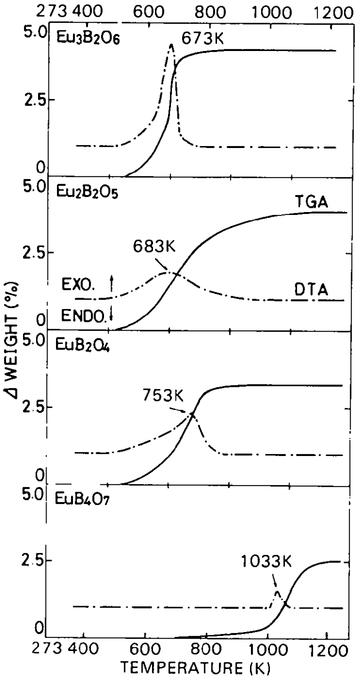

Fig. 4. Thermogravimetric analysis (TGA) and differential thermal analysis (DTA) curves for Eu^{II} borates.

strong function of the interatomic Eu^{2+} spacing and Eu^{2+}–O^{2-}–Eu^{2+} angle. The interatomic distances between neighboring Eu^{2+} ions in EuB_4O_7 are very long compared with other Eu^{II} compounds with unique magnetic properties (Greedan & McCarthy, 1972), *e.g.* EuO (3·63 Å for six nearest neighbors and 5·14 Å for twelve next-nearest neighbors), and are insufficient for magnetic interactions. This reflects the observation that EuB_4O_7 is a paramagnet, obeying the Curie–Weiss law.

The tetraborate, EuB_4O_7, has been found to give a strong emission based on the $4f^7$–$4f^65d$ transition of the Eu^{2+} ion (Machida, Adachi & Shiokawa, 1979*a*), and its luminescence properties are summarized together with those of other Eu^{II} borates in Table 5. Whereas no emission is observed in $Eu_3B_2O_6$ and $Eu_2B_2O_5$, two other borates, EuB_2O_4 and EuB_4O_7, give similar emissions to each other which have the same half-width value (20 nm) and peak at about 370 nm. In particular, it is noticeable that the quantum efficiency for the emission band of EuB_4O_7 is very high (about 7%) compared with those of other Eu^{II} borates in spite of a concentration quenching effect: a compound diluted with Sr^{2+} ions, $Sr_{0\cdot95}Eu_{0\cdot05}B_4O_7$, has a value of about 40% under 254 nm excitation at 300 K. This corresponds to the thermal stabilities resulting from the differences in structural frameworks. One of the quenching effects of Eu^{2+}-activated phosphors is considered as a non-radiative process proceeding by repetition of the energy transfer *via* a dipole–dipole interaction between neighboring Eu^{2+} ions (Dexter, 1953; Blasse, 1969). Consequently the Eu^{2+} ions in EuB_4O_7, which are located in the 'cages' of BO_4 units, can hardly be able to interact with neighboring Eu^{2+} ions, and hence EuB_4O_7 gives the strong emission. Since the peak positions of emission bands of Eu^{2+}-activated phosphors strongly depend on the crystal fields formed by anions around an Eu^{2+} ion, the fact that EuB_2O_4 and EuB_4O_7 give similar emissions to each other may be due to the similarities of their Eu^{2+} coordination numbers [8 for EuB_2O_4 (Machida, Adachi & Shiokawa, 1979*b*) and 9 for EuB_4O_7].

Table 5. *Luminescence properties for* Eu^{II} *borates*

Compound	λ_{max} (nm)*	$\lambda/2$ (nm)†	QE (%)‡
$Eu_3B_2O_6$	–	–	–
$Eu_2B_2O_5$	–	–	–
EuB_2O_4	370	20	negligible
EuB_4O_7	372	20	7

* λ_{max} = positions of the maximum of the emission band.
† $\lambda/2$ = Half-width of the emission band.
‡ QE = Quantum efficiency under 254 nm excitation at 300 K.

The authors wish to thank Drs N. Kasai, N. Yasuoka and N. Tanaka, and Mr K. Miki for their helpful suggestions. The computations were carried out at the Crystallographic Research Center of the Institute for Protein Research, Osaka University.

References

Ashida, T. (1973). *The Universal Crystallographic Computing System – Osaka*, pp. 55–61. The Crystallographic Research Center of the Institute for Protein Research, Osaka Univ., Japan.

Blasse, G. (1969). *Philips Res. Rep.* **24**, 131–144.

Dexter, D. L. (1953). *J. Chem. Phys.* **21**, 836–850.

Felsche, J. & Kaldis, E. (1972). *J. Solid State Chem.* **5**, 49–56.

Greedan, J. E. & McCarthy, G. J. (1972). *Mater. Res. Bull.* **7**, 531–542.

Hata, H., Adachi, G. & Shiokawa, J. (1977). *Mater. Res. Bull.* **12**, 811–814.

International Tables for X-ray Crystallography (1974). Vol. IV. Birmingham: Kynoch Press.

McCarthy, G. J. & White, W. B. (1970). *J. Less-Common Met.* **22**, 409–417.

McGuire, T. R. & Shafer, M. W. (1964). *J. Appl. Phys.* **35**, 984–988.

McGuire, T. R., Shafer, M. W., Joenk, R. J., Alperin, H. A. & Pickart, S. J. (1966). *J. Appl. Phys.* **37**, 981–982.

Machida, K., Adachi, G. & Shiokawa, J. (1979*a*). *J. Lumin.* **21**, 101–110.

Machida, K., Adachi, G. & Shiokawa, J. (1979*b*). *Acta Cryst.* B**35**, 149–151.

Machida, K., Hata, H., Okuno, K., Adachi, G. & Shiokawa, J. (1979). *J. Inorg. Nucl. Chem.* **41**, 1425–1430.